



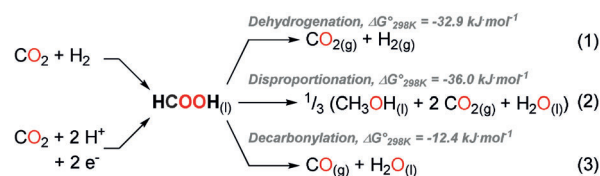
Transition-Metal-Free Acceptorless Decarbonylation of Formic Acid Enabled by a Liquid Chemical-Looping Strategy

Arnaud Imberdis, Guillaume Lefèvre, and Thibault Cantat*

Abstract: The selective decarbonylation of formic acid was achieved under transition-metal-free conditions. Using a liquid chemical-looping strategy, the thermodynamically favored dehydrogenation of formic acid was shut down, yielding a pure stream of CO with no H₂ or CO₂ contamination. The transformation involves a two-step sequence where methanol is used as a recyclable looping agent to yield methylformate, which is subsequently decomposed to carbon monoxide using alkoxides as catalysts.

Among C1 chemicals, formic acid (HCOOH, FA) has been the focus of renewed interests since it is an important product in catalytic transformations related to the storage of sustainably produced energy. Recent efforts have indeed showed that HCOOH is a key intermediate in the hydrogenation of CO₂ to methanol and methane.^[1] In addition, formic acid can be produced from the (photo)electrolysis of CO₂ or the hydrogenation of CO₂ and carbonates.^[2a-c] Despite its simple formulation, FA can undergo different decomposition reactions depending on the reaction conditions and the presence of catalysts. While homogeneous catalysts have been developed that can disproportionate FA to methanol, the main decomposition pathway involves the dehydrogenation of HCOOH to H₂ and CO₂.^[3a-e] In fact, the reversible hydrogenation of CO₂ (and bicarbonates) to formates has led to the concept of a hydrogen battery for the storage of H₂ in liquid form.^[4]

From a thermodynamic standpoint, FA could also decompose to CO and H₂O, with a Gibbs free energy of $-12.4 \text{ kJ mol}^{-1}$ at 298 °C (Scheme 1).^[5] This decarbonylation reaction is less favoured than the classical dehydrogenation ($\Delta G^\circ = -32.9 \text{ kJ mol}^{-1}$ at 298 °C);^[5] but it would provide a convenient flow of CO from a renewable feedstock. Utilized in large scale in the Fischer–Tropsch and Cativa processes,^[6] as well as in hydroformylation reactions, carbon monoxide is currently produced from fossil sources, primarily through methane steam reforming (SMR) or autothermal reformer (ATR).^[7] Alternatively, the reverse water–gas shift (RWGS) reaction can convert CO₂ and H₂ into a mixture of CO, H₂O, CO₂, and H₂ at equilibrium.^[8] Overall, these methods suffer from severe disadvantages, such as the need for further purification of the gas stream, to separate CO. In this context,



Scheme 1. Routes for the production and decomposition of formic acid.

the production of CO from FA would afford an attractive way to produce a stream of pure CO, in a controlled way, from a sustainable and storable precursor.^[9]

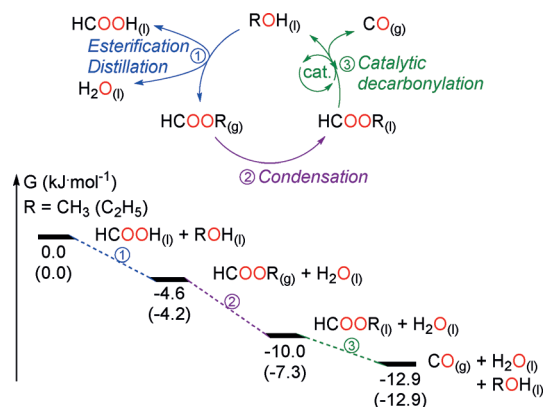
In situ decomposition of formic acid to promote for example formal carbonylation or hydroxycarbonylation, for example, has been reported.^[10] Only a few methods have been developed to promote the acceptorless decarbonylation of FA, which relied on the use of stoichiometric amounts of sulfuric or phosphoric acids^[11] or on thermolytic conditions.^[12] Catalytic strategies are scarce. These involve zeolite-based catalysts able to decompose FA at high temperatures ($> 150^\circ\text{C}$), to remove water, and exhibit modest activity with turnover frequencies up to 39 h^{-1} .^[13] Very recently, while exploring the alkoxycarbonylation of alkenes with FA, Beller et al. discovered that palladium complexes, supported by chelating bis-phosphines decorated with pyridine bases, could catalyze the acceptorless decarbonylation of FA.^[14] Because the dehydrogenation of HCOOH is facile, both thermodynamically and kinetically, the authors noted the concomitant release of at least 10 % CO₂ and H₂. In the pursuit of a practical system able to selectively decarbonylate FA, we sought a transition-metal-free method. Under organocatalytic conditions, the dehydrogenation of HCOOH is indeed difficult and only a handful of catalysts have been shown to decompose FA to CO₂ and H₂.^[15] Herein, we report a system that combines chemical looping and an organocatalytic transformation for the decomposition of FA into CO and H₂O, without the formation of H₂, at low temperature ($< 75^\circ\text{C}$).

From a mechanistic standpoint, the decarbonylation of FA must involve a C–H activation step that results in formal deprotonation of the C–H group to reduce the carbon atom. Computationally, the corresponding proton has a $\text{p}K_{\text{a}}$ of ca. 31.^[16] The direct decarbonylation of HCOOH with an organic Brønsted base is hence illusory in the presence of the more acidic O–H functionalities of FA ($\text{p}K_{\text{a}} = 3.7$) or water. To circumvent this limitation, we envisioned a chemical-looping strategy. Chemical looping is a powerful and practical approach where a transformation is divided into several sub-reactions in order to separate gases, prevent deleterious

*A. Imberdis, Dr. G. Lefèvre, Dr. T. Cantat
NIMBE, CEA, CNRS, Université Paris-Saclay, CEA Saclay
91191 Gif-sur-Yvette cedex (France)
E-mail: thibault.cantat@cea.fr

Supporting information and the ORCID identification number(s) for the author(s) of this article can be found under:
<https://doi.org/10.1002/anie.201909039>.

equilibria, and/or avoid incompatible substrates. This has been applied using solid looping agents in a variety of processes, including the RWGS reaction, the (super-)dry reforming of methane, and CO₂ capture from combustion.^[17] An esterification reaction is well-suited to separate the acidic O-H functionalities from the C-H bond in Equation (3) because it would yield an alkylformate derivative with a Gibbs free energy intermediate between FA and CO + H₂O (Scheme 2). An alcohol was hence chosen to set up the



Scheme 2. Principle of liquid chemical looping for the transition-metal-free decarbonylation of formic acid, with the associated Gibbs free energies using methanol and ethanol as looping reagents.

chemical looping depicted in Scheme 2. This relies on the esterification of formic acid with an alcohol and isolation of the corresponding alkylformate by distillation (steps 1–2 in Scheme 2). The subsequent catalytic decarbonylation of the alkylformate would afford a stream of CO, while regenerating the alcohol. The choice of the best-suited looping agent is discussed at the end on this communication since it relies both on the physicochemical properties of the alcohol/alkylformate couple and on the reactivity of the alkylformate in the decarbonylation step.

Interestingly, several metal catalysts have been reported for the acceptorless decarbonylation of alkylformates based on copper,^[18a] ruthenium,^[18b] rhodium,^[18c] osmium,^[18d] and palladium^[18e] complexes that are able to oxidatively add to the formate C-H bond. Organic alternatives exist, which involve guanidines,^[19] amines, or phosphines.^[20] All these catalysts nevertheless operate at elevated temperatures, above 140 °C. Reasoning that an alkoxide base (pK_a = 29–32 in DMSO)^[21] would be basic enough to deprotonate a C-H bond of a formate group, a DMF solution of methylformate (MF) was investigated, in the presence of 5.0 mol % potassium methoxide (MeOK). In a sealed NMR tube, rapid decomposition of 56 % MF was noted after 3 h at 19 °C in DMF (Entry 6, Table 1). The concomitant formation of methanol was observed by ¹H and ¹³C NMR spectroscopy, while the production of CO was identified in the gas phase using GC. Importantly, neither H₂ nor CO₂ was detected by GC in the gas phase. A conversion of 85 % was reached at 75 °C, while no reaction occurred in the absence of the catalyst. Encouraged by this success, the influence of the

Table 1: Scope of the reaction for the decarbonylation of alkyl formate.^[a]

$\text{HCOOR} \xrightarrow{\text{R'XM (5 mol\%)}} \text{CO} + \text{ROH}$					
Conversion (%) ^{[b][c]}					
Entry	R	R'XM	T [°C]	t [h]	Conv [%] ^[c]
1		None	30	20	< 5
2		MeOLi	30	8	54
3		MeONa	19	3	< 5
4		MeONa/18C6	19	3	56
5		MeONa	30	3	46
6		MeOK	19 (75)	3	56 (85)
7	Me	MeOK/18C6	19	3	47
8		MeOK/222	19	3	49
9		MeORb	19	3	44
10		EtOK	19	3	45
11		tBuOK	30	3	59
12		Me ₂ NLi	19	20	42
13		TBDNa	30	3	56
14		TBDK	19	4	50
15	Et	MeOK	19 (75)	2	24 (77)
16		EtOK	19	1	51
17	nBu	tBuOK	30 (75)	3	60 (81)
18	Bz	MeOK	19 (75)	3	69 (94)

[a] Reaction conditions: 1 mmol MF, 50 μmol catalyst (5 mol %), 500 μL DMF. [b] Screening of the solvent (see details in the Supporting Information). [c] Determined by ¹H NMR of the crude reaction mixture.

catalyst, the solvent, and the alkylformate were investigated (Table 1). Given the low exergonicity of the decarbonylation of MF ($\Delta G^\circ_{298\text{K}} = -2.9 \text{ kJ mol}^{-1}$), the reaction operates under an equilibrium and, in a sealed NMR tube, a maximum conversion of 60 % was evaluated for the decomposition of MF vs. 90 % at 75 °C, which is in agreement with an endothermic reaction ($\Delta H^\circ_{298\text{K}} = +36.9 \text{ kJ mol}^{-1}$). A screening of solvents revealed that the decarbonylation of MF was efficient in polar aprotic solvents with large dissociation constants, such as DMF ($\epsilon = 36.7$) and NMP ($\epsilon = 32.2$), with a conversion to CO and methanol of 56 and 58 %, respectively, after 3 h at 19 °C (see Table S1 in the Supporting Information). Importantly, the decarbonylation was completely shut down in methanol and in neat conditions, thereby indicating potential poisoning or deactivation of the catalyst by both the product and the substrate.

While MeOLi and MeONa were found to be inactive at 19 °C, these catalysts decompose MF to CO and methanol at 30 °C, and a longer reaction time was required in the presence of the lithium derivative (8 vs. 3 h; Entries 2, 3 and 5 in Table 1). The rubidium salt MeORb exhibited catalytic activity close to that of MeOK (Entry 9 in Table 1). Since alkali metal cations have been shown to influence the performances of catalytic systems through coordination to oxygen-rich substrates, the coordination sphere of the potassium cation in MeOK was modulated by the addition of exogenous chelating ligands. Addition of 5.0 mol % of the 18-C-6 crown ether or the 2,2,2-cryptand had no impact on the catalytic performances of MeOK, thus suggesting an innocent

role of K^+ . The difference in reactivity between MeOK and its lithium and sodium congeners hence likely stems from the tighter ion pairs formed between the MeO^- anion and the hard Li^+ and Na^+ cations. This trend is reflected in the shortening of O–M bond length in the alkali oxides M_2O from 2.9, 2.8, 2.4, to 2.0 Å across the series Rb, K, Na, Li.^[22] This interpretation is supported by the comparable catalytic activities of MeOK and MeONa/18-C-6 at 19°C (Entries 4 and 6 in Table 1). It is notable that bases stronger than MeOK, such as EtOK, *t*-BuOK, and nitrogen-containing bases (TBDK), exhibited catalytic performances similar to MeOK; similarly, Me_2NLi behaved like MeOLi.

Bulkier ethyl and *n*-butyl formates were found to be less reactive than MF and required stronger bases as catalysts (entries 15–17). In contrast, 94 % of the more activated benzyl formate was decomposed at 75°C. It is noteworthy that all the results displayed in Table 1 involved very mild temperatures (19°C or 30°C).

To suppress the thermodynamic constraint associated with pressure buildup in a closed vessel, the decomposition of MF was carried out in an open system and monitored using a eudiometer (Figure 1). Using the reaction conditions of Entry 6, Table 1, CO was generated in 82% yield after only 50 min at 19°C (red plot in Figure 1). The setup enabled a kinetic study, thereby establishing that the rate law is first order in catalyst and has a -1 order with respect to MeOH while the order for MF is non-integer (see the Supporting Information).

These data confirm that both MF and MeOH have a detrimental effect on the reactivity of the catalyst and, to better comprehend this behavior, DFT calculations were carried out on the mechanism of the decarbonylation reaction.

The MeO^- catalyst is a base strong enough to interact with MF, and although the deprotonation of the C–H bond is slightly uphill ($\Delta G = +5.1$ kcal mol⁻¹), CO release occurs readily via a low lying transition state (TS_2 , $\Delta G = +8.1$ kcal mol⁻¹; Scheme 3, green surface). Interestingly, the methanol byproduct forms a strong H-bond with MeO^- and the separation of the free MeO^- base from methanol requires $+7.3$ kcal mol⁻¹. As a result, the energy span governing the activity of the MeO^- catalyst reaches 15.4 kcal mol⁻¹.

As the reaction proceeds, the accumulation of methanol can be accounted for, mechanistically, by exploring the catalytic behavior of the H-bonded $[MeO^{\cdots}HOME]$ pair (blue surface in Scheme 3). The decreased basicity of the catalyst results in destabilization of the two transition states responsible for the deprotonation of the C–H bond in MF and the release of CO from the $CH_3OC(O)^-$ anion (e.g., TS_2 , $\Delta G = +14.5$ kcal mol⁻¹). As a consequence, in the presence of methanol, the reaction span increases to 19.8 kcal mol⁻¹, thereby explaining the deleterious influence of the reaction product on the catalyst activity. In addition, the presence of a large excess MF results in the trapping of the MeO^- catalyst to form a $HC(OMe)_2O^-$ anion (with a Gibbs free energy of -3.7 kcal mol⁻¹), thereby slowing down the rate of the decarbonylation.

Based on these key findings, an optimized system was found for the decarbonylation of formic acid, using the

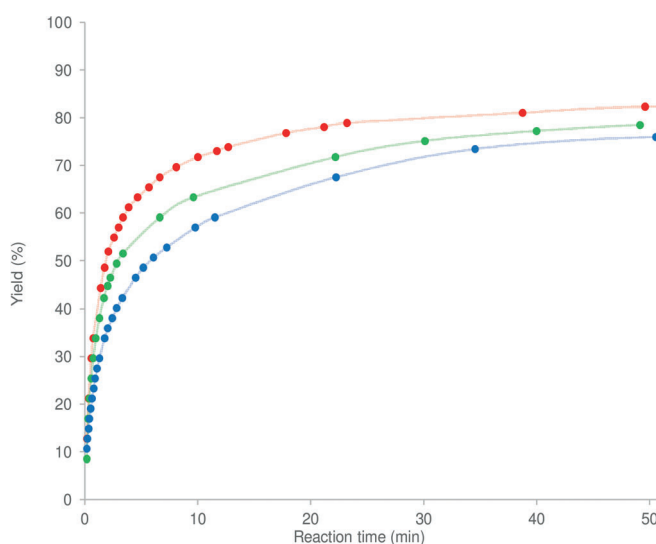
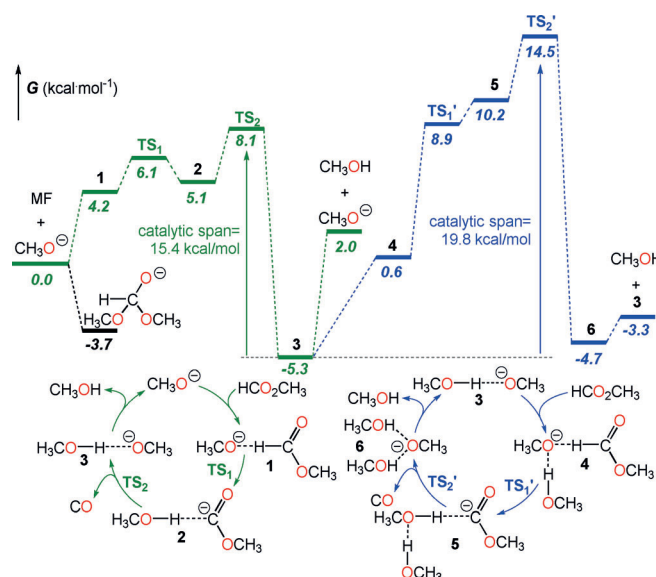
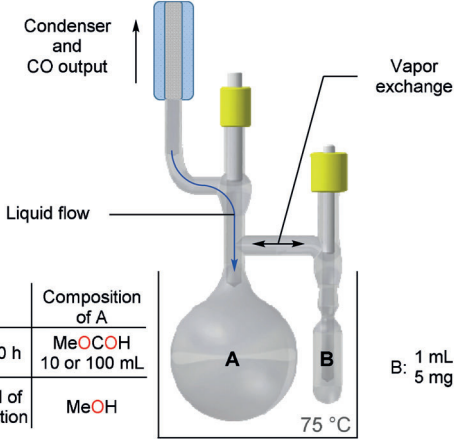


Figure 1. Plot of the volume of CO produced upon decarbonylation of methyl formate in an open system using different initial loadings of MeOH (red: 0 mol% MeOH, green: 5 mol% MeOH, blue: 10 mol% MeOH) and evolution of the rate constant with respect to the initial concentration of MeOK and MeOH.

chemical looping depicted in Scheme 2. MeOH/MF was selected as the best looping system, because both MeOH and MF are liquids under ambient conditions and MF presents a high CO content of 47 wt %. Using a two-chamber system depicted in Table 2, a solution of MeOK in DMF (0.07 mol L⁻¹) was connected to a vessel containing pure MF. The device was equipped with a condenser and immersed in a 75°C oil bath. Thanks to the low boiling points of MF and MeOH of 32 and 61°C, respectively, accumulation of the reagents and products in the solution containing the catalyst (chamber B in Table 2) is avoided and methanol is collected in



Scheme 3. Decarbonylation of methyl formate catalyzed by MeO^- . Gibbs free energies in kcal mol⁻¹ computed at the M062x/6-311++G**/PCM level of theory.

Table 2: Catalytic decarbonylation of MF using a two-chamber setup.^[a]


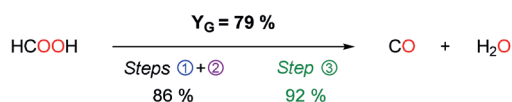
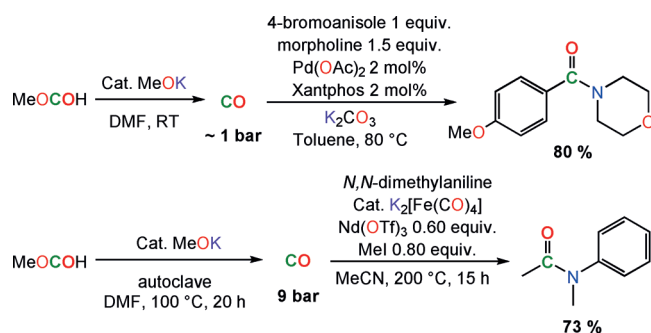
Entry	Reagent (mL/mol)	t	TON ^[b]	TOF (h ⁻¹) ^[b]	Yield [%] ^[b]
1	MeOCOH 10/0.16	20 h	1618	81	70
2	MeOCOH 10/0.16	40 h	2171	54	92
3	MeOCOH 100/1.6	4 d	5000	52	22

[a] Reaction conditions: In a two-chamber system surmounted with a cooler, pure MF is introduced in the reserve chamber (A) and the catalytic chamber (B) is charged with 7 μ mol catalyst (5 mg) and 1 mL DMF. The setup is immersed in an oil bath at 75 °C. [b] Determined by ¹H NMR of an aliquot of compartment A mixture.

the reservoir vessel (chamber A). Using this setup, an excellent TON of 5000 was measured, with a TOF up to 81 h⁻¹ at 75 °C. Overall, 10 mL MF were successfully decarbonylated in 92 % yield to afford 3.7 L CO, after 40 h (Table 2). 6.1 mL of methanol were recovered, with a purity of 96 % (along with 4 % unreacted MF). To demonstrate the liquid chemical looping depicted in Scheme 2, the regeneration of MF was carried out by esterification of the produced methanol with HCOOH at 32 °C. Continuous distillation of MF enabled the isolation of the alkylformate in 86 % yield after 5 h, thanks to the absence of azeotrope between MF and formic acid, water, or methanol.

All together, the decarbonylation of formic acid to CO and water was achieved in 79 % yield at low temperature (75 °C), using transition-metal-free catalysts, for the first time (Scheme 4). No H₂ nor CO₂ contamination of the gas stream was detected by GC, although the dehydrogenation of formic acid is thermodynamically preferred.

Recently, several surrogates of CO have been designed to generate a low pressures of CO for synthesis at the laboratory scale, for instance using two-chamber systems (e.g., COgen).^[23] Similarly, we were able to perform the gram-scale aminocarbonylation of 4-bromoanisole with morpholine, using CO produced from MF (Scheme 5).^[24] The absence of H₂ circumvented the dehalogenation of the arylbromide in

**Scheme 4.** Global process (Y_G = global yield of the process).**Scheme 5.** Tandem carbonylation reactions enabling the preparation of amides with CO generated from MF.

this palladium-catalyzed reaction. Interestingly, the possibility of generating high pressures of CO (up to 26 bars, allowed iron-catalyzed carbonylation of the N-CH₃ bond in N,N-dimethylaniline in 73 % yield under 9 bars of CO, using a double autoclave system (see Scheme 5 and the Supporting Information).^[25] While chemical looping is common strategy in the realm of heterogeneous catalysis, the present work hence exemplifies how liquid chemical looping can unlock thermodynamically unfavored transformations, at low temperatures, without the need for sophisticated metal catalysts.

Acknowledgements

The authors acknowledge for financial support of this work: CEA, CNRS, CINES (project sis6494), the CHARMMAT Laboratory of Excellence, and the European Research Council (ERC Consolidator Grant Agreement no. 818260).

Conflict of interest

The authors declare no conflict of interest.

Keywords: carbon monoxide · chemical looping · decarbonylation · formic acid · organocatalysis

- [1] a) S. Wesselbaum, V. Moha, M. Meuresch, S. Brosinski, K. M. Thenert, J. Kothe, T. vom Stein, U. Englert, M. Hölscher, J. Klankermayer, et al., *Chem. Sci.* **2015**, 6, 693–704; b) M. Behrens, F. Studt, I. Kasatkin, S. Kuhl, M. Havecker, F. Abild-Pedersen, S. Zander, F. Girgsdies, P. Kurr, B.-L. Kniep, et al., *Science* **2012**, 336, 893–897.
- [2] a) A. S. Agarwal, Y. Zhai, D. Hill, N. Sridhar, *ChemSusChem* **2011**, 4, 1301–1310; b) C. Federsel, R. Jackstell, M. Beller, *Angew. Chem. Int. Ed.* **2010**, 49, 6254–6257; *Angew. Chem.* **2010**, 122, 6392–6395; c) C. Federsel, C. Ziebart, R. Jackstell, W. Baumann, M. Beller, *Chem. Eur. J.* **2012**, 18, 72–75.
- [3] a) A. J. M. Miller, D. M. Heinekey, J. M. Mayer, K. I. Goldberg, *Angew. Chem. Int. Ed.* **2013**, 52, 3981–3984; *Angew. Chem.* **2013**, 125, 4073–4076; b) S. Savourey, G. Lefèvre, J.-C. Berthet, P. Thuéry, C. Genre, T. Cantat, *Angew. Chem. Int. Ed.* **2014**, 53, 10466–10470; *Angew. Chem.* **2014**, 126, 10634–10638; c) M. C.

- Neary, G. Parkin, *Chem. Sci.* **2015**, 6, 1859–1865; d) K. Sordakis, A. Tsurusaki, M. Iguchi, H. Kawanami, Y. Himeda, G. Laurenczy, *Green Chem.* **2017**, 19, 2371–2378; e) A. Tsurusaki, K. Murata, N. Onishi, K. Sordakis, G. Laurenczy, Y. Himeda, *ACS Catal.* **2017**, 7, 1123–1131.
- [4] a) A. Boddien, F. Gärtner, C. Federsel, P. Sponholz, D. Mellmann, R. Jackstell, H. Junge, M. Beller, *Angew. Chem. Int. Ed.* **2011**, 50, 6411–6414; *Angew. Chem.* **2011**, 123, 6535–6538; b) K. Sordakis, C. Tang, L. K. Vogt, H. Junge, P. J. Dyson, M. Beller, G. Laurenczy, *Chem. Rev.* **2018**, 118, 372–433.
- [5] T. Zell, R. Langer, *Phys. Sci. Rev.* **2018**, 3, 57–93.
- [6] J. H. Jones, *Platinum Met. Rev.* **2000**, 44, 94–105.
- [7] I. Dybkjaer, *Fuel Process. Technol.* **1995**, 42, 85–107.
- [8] F. D. Doty, G. N. Doty, J. P. Staab, L. L. Holte, *ES2010-90362 ASME conference*, **2010**, 1–10.
- [9] a) J. Klankermayer, S. Wesselbaum, K. Beydoun, W. Leitner, *Angew. Chem. Int. Ed.* **2016**, 55, 7296–7343; *Angew. Chem.* **2016**, 128, 7416–7467; b) W. Supronowicz, I. A. Ignatyev, G. Lolli, A. Wolf, L. Zhao, L. Mleczko, *Green Chem.* **2015**, 17, 2904–2911.
- [10] a) X. Qi, C.-L. Li, X.-F. Wu, *Chem. Eur. J.* **2016**, 22, 5835–5838; b) F.-P. Wu, J.-B. Peng, X. Qi, X.-F. Wu, *Catal. Sci. Technol.* **2017**, 7, 4924–4928; c) J.-P. Simonato, *J. Mol. Catal. A* **2003**, 197, 61–64; d) T. G. Ostapowicz, M. Schmitz, M. Krystof, J. Klankermayer, W. Leitner, *Angew. Chem. Int. Ed.* **2013**, 52, 12119–12123; *Angew. Chem.* **2013**, 125, 12341–12345.
- [11] J. S. Morgan, *J. Chem. Soc. Trans.* **1916**, 109, 274–283.
- [12] W. L. Nelson, C. J. Engelder, *J. Phys. Chem.* **1925**, 30, 470–475.
- [13] P. Losch, A. S. Felten, P. Pale, *Adv. Synth. Catal.* **2015**, 357, 2931–2938.
- [14] R. Sang, P. Kucmierczyk, K. Dong, R. Franke, H. Neumann, R. Jackstell, M. Beller, *J. Am. Chem. Soc.* **2018**, 140, 5217–5223.
- [15] C. Chauvier, A. Tlili, C. Das Neves Gomes, P. Thuéry, T. Cantat, *Chem. Sci.* **2015**, 6, 2938–2942.
- [16] The pK_a -values were calculated with respect to the furan anion as reference base (experimental value of 35) according to the formula: $pK_a(\text{THF}) = 35 + \Delta G / (2.303 RT)$ (ΔG in kcal mol^{-1} and T in K); K. Shen, Y. Fu, J.-N. Li, L. Liu, Q.-X. Guo, *Tetrahedron Lett.* **2007**, 63, 1568–1576.
- [17] a) M. Keller, J. Fung, H. Leion, T. Mattisson, *Fuel* **2016**, 180, 448–456; b) M. Wenzel, L. Rihko-Struckmann, K. Sundmacher, *Chem. Eng. J.* **2018**, 336, 278–296; c) T. Pröll, P. Kolbitsch, J. Bolhär-Nordenkamp, H. Hofbauer, *AIChE J.* **2009**, 55, 3255–3266; d) M. Ryden, A. Lyngfelt, *Int. J. Hydrogen Energy* **2006**, 31, 1271–1283; e) M. M. Hossain, H. I. de Lasa, *Chem. Eng. Sci.* **2008**, 63, 4433–4451.
- [18] a) G. Doyle, US Pat. 4.319.050, **1981**; b) G. Jenner, E. M. Nahmed, H. Leismann, *Tetrahedron Lett.* **1989**, 30, 6501–6502; c) H. A. Zahalka, H. Alper, *Tetrahedron Lett.* **1987**, 28, 2215–2216; d) C. Legrand, Y. Castanet, A. Mortreux, F. Petit, *Tetrahedron Lett.* **1992**, 33, 3753–3756; e) J. S. Lee, J. C. Kim, Y. G. Kim, *Appl. Catal.* **1990**, 57, 1–30.
- [19] M. J. Green, Eur Pat. EP0115387, **1984**.
- [20] F. R. Vega, J. C. Clément, H. des Abbayes, *Tetrahedron Lett.* **1993**, 34, 8117–8118.
- [21] W. N. Olmstead, Z. Margolin, F. G. Bordwell, *J. Org. Chem.* **1980**, 45, 3295–3299.
- [22] N. K. McGuire, M. O’Keeffe, *J. Solid State Chem.* **1984**, 54, 49–53.
- [23] a) C. Veryser, S. Van Mileghem, B. Egle, P. Gilles, W. M. De Borggraeve, *React. Chem. Eng.* **2016**, 1, 142–146; b) C. Veryser, G. Steurs, L. Van Meervelt, W. M. De Borggraeve, *Adv. Synth. Catal.* **2017**, 359, 1271–1276; c) S. D. Friis, A. T. Lindhardt, T. Skrydstrup, *Acc. Chem. Res.* **2016**, 49, 594–605.
- [24] J. R. Martinelli, D. A. Watson, D. M. M. Freckmann, T. E. Barder, S. L. Buchwald, *J. Org. Chem.* **2008**, 73, 7102–7107.
- [25] T. Nasr Allah, S. Savourey, J.-C. Berthet, E. Nicolas, T. Cantat, *Angew. Chem. Int. Ed.* **2019**, 58, 10884–10887; *Angew. Chem.* **2019**, 131, 11000–11003.

Manuscript received: July 19, 2019

Revised manuscript received: September 10, 2019

Accepted manuscript online: September 17, 2019

Version of record online: ■■■■■, ■■■■■

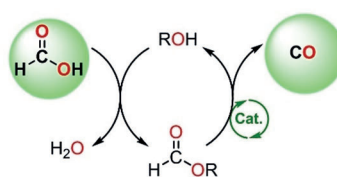
Communications



Organocatalysis

A. Imberdis, G. Lefèvre,
T. Cantat* ————— ■■■-■■■

Transition-Metal-Free Acceptorless
Decarbonylation of Formic Acid Enabled
by a Liquid Chemical-Looping Strategy



- ✓ Transition-metal-Free
- ✓ Acceptor-less decarbonylation
- ✓ No H₂ and CO₂ contamination
- ✓ Low temperature

In the loop: Selective and acceptorless decarbonylation of formic acid was achieved for the first time under transition-metal-free conditions. The approach, inspired by chemical-looping strategies,

shuts down the thermodynamically favored dehydrogenation of formic acid, yielding a pure stream of CO without H₂ or CO₂ contamination.